Nanosecond Retinal Structure Changes in K-590 During the Room-Temperature Bacteriorhodopsin Photocycle: Picosecond Time-Resolved Coherent Anti-Stokes Raman Spectroscopy

Olaf Weidlich, Laszlo Ujj, Frank Jäger, and G. H. Atkinson
Department of Chemistry and Optical Sciences Center, University of Arizona, Tucson, Arizona 85721 USA

ABSTRACT Time-resolved vibrational spectra are used to elucidate the structural changes in the retinal chromophore within the K-590 intermediate that precedes the formation of the L-550 intermediate in the room-temperature (RT) bacteriorhodopsin (BR) photocycle. Measured by picosecond time-resolved coherent anti-Stokes Raman scattering (PTR/CARS), these vibrational data are recorded within the 750 cm^{-1} to 1720 cm^{-1} spectral region and with time delays of 50–260 ns after the RT/BR photocycle is optically initiated by pulsed (<3 ps, 1.75 nJ) excitation. Although K-590 remains structurally unchanged throughout the 50-ps to 1-ns time interval, distinct structural changes do appear over the 1-ns to 260-ns period. Specifically, comparisons of the 50-ps PTR/CARS spectra with those recorded with time delays of 1 ns to 260 ns reveal 1) three types of changes in the hydrogen-out-of-plane (HOOP) region: the appearance of a strong, new feature at 984 cm^{-1}; intensity decreases for the bands at 957 cm^{-1}, 952 cm^{-1}, and 939 cm^{-1}; and small changes in intensity and/or frequency of bands at 855 cm^{-1} and 805 cm^{-1}; and 2) two types of changes in the C-C stretching region: the intensity increase in the band at 1196 cm^{-1} and small intensity changes and/or frequency shifts for bands at 1300 cm^{-1} and 1362 cm^{-1}. No changes are observed in the C=C stretching region, and no bands assignable to the Schiff base stretching mode (C=NH^+) mode are found in any of the PTR/CARS spectra assignable to K-590. These PTR/CARS data are used, together with vibrational mode assignments derived from previous work, to characterize the retinal structural changes in K-590 as it evolves from its 3.5-ps formation (ps/K-590) through the nanosecond time regime (ns/K-590) that precedes the formation of L-550. The PTR/CARS data suggest that changes in the torsional modes near the C_{14}-C_{15}=N bonds are directly associated with the appearance of ns/K-590, and perhaps with the KL intermediate proposed in earlier studies. These vibrational data can be primarily interpreted in terms of the degree of twisting of the C_{14}-C_{15} retinal bond. Such twisting may be accompanied by changes in the adjacent protein. Other smaller, but nonetheless clear, spectral changes indicate that alterations along the retinal polyene chain also occur. The changes in the retinal structure are preliminary to the deprotonation of the Schiff base nitrogen during the formation of M-412. The time constant for the ps/ns K-590 transformation is estimated from the amplitude change of four vibrational bands in the HOOP region to be 40–70 ns.

INTRODUCTION

The structural changes in the retinal chromophore found in the transmembrane protein bacteriorhodopsin (BR) (*Halobacterium salinarium*) have long been associated with the transduction and utilization of absorbed light energy for the ATP synthesis resulting from its room-temperature (RT) photocycle (for recent reviews see Birge, 1990; Mathies et al., 1991; Oesterhelt et al., 1992; Rothschild, 1992; Ebrey, 1993; Krebs and Khorana, 1993; Althaus et al., 1995; Lanyi and Váró, 1995; Maeda, 1995). Chemically, the RT/BR photocycle functions to pump protons across the cell membrane, thereby creating the chemical potential required to energetically drive ATP synthesis (Oesterhelt and Stoeckenius, 1974). Optical absorption in RT/BR creates an excited electronic state population (~500 fs lifetime) (Sharkov et al., 1985; Nuss et al., 1985; Petrich et al., 1987; Mathies et al., 1988; van den Berg, 1990; reviewed in Kochendoerfer and Mathies, 1995), whereas the remainder of the photocycle (i.e., formation of the intermediates K-590, L-550, M-412, N-560, and O-640) occurs on ground-state potential surfaces. The energetic driving force (chemical potential) for the RT/BR photocycle is derived from changes (structural and/or electrostatic) in the retinal chromophore, its surrounding protein environment, or both.

Spectroscopically, particular attention has been given to changes in the retinal structure during the initial 100 ps of the RT/BR photocycle when K-590 is present (Sharkov et al., 1985; Nuss et al., 1985; Polland et al., 1986; Petrich et al., 1987; Dobler et al., 1988; Doig et al., 1991; Diller et al., 1995). The formation of K-590 is known to involve all-*trans* to 13-*cis* retinal isomerization. The retinal structural changes, as well as the changes in the surrounding protein, that occur after K-590 formation, but before its transformation to L-550 (~1 μs time constant) (e.g., Váró and Lanyi, 1991; Lozier et al., 1992), however, remain only partially understood. It is especially important to note that the duration of the optical excitation used to initiate the RT/BR photocycle plays an important role. Ideally, excitation should be shorter than the excited electronic-state lifetime (i.e., <500 fs for BR) to avoid any secondary photochem-

Received for publication 19 November 1996 and in final form 3 February 1997.

Address reprint requests to Dr. George H. Atkinson, Department of Chemistry, University of Arizona, P.O. Box 20041, Tucson, AZ 85721-0041. Tel.: 520-621-6293; Fax: 520-621-4858; E-mail: atkinson@ccit.arizona.edu.

0006-3495/97/05/2329/13 $2.00

istry resulting from absorption by photocycle intermediates (e.g., K-590).

Changes in K-590 during the 50-ps to 1-μs interval of the RT/BR photocycle have been derived from data measured as 1) time-resolved absorption, 2) time-resolved fluorescence, 3) low-temperature (LT) infrared (IR), and 4) time-resolved RT vibrational (RR and IR) data.

1. Small variations in the visible absorption spectrum assigned to K-590 have been reported to appear in the nanosecond time regimen (Milder and Kliger, 1988; Shichida et al., 1983). The kinetics associated with these absorption changes have also been measured (time constants of ~10 ns (Milder and Kliger, 1988) and <150 ns (Shichida et al., 1983)). These spectroscopic and kinetic changes have been used to identify a distinct intermediate, termed KL. Because the excitation conditions used in these experiments vary considerably with respect to pulsewidth (4 ns versus 25 ps) and pulse energy, however, it is difficult to compare these results directly.

Transient absorption experiments utilizing <10-ps excitation of RT/BR found neither spectroscopic nor kinetic data with which to identify KL (Delaney et al., 1993; Yamamoto et al., 1994). It has been suggested, therefore, that the previously observed absorption differences may be associated with secondary photochemistry and/or BR photocycle back-reactions that are not part of the normal RT/BR photocycle (Delaney et al., 1993; Yamamoto et al., 1994).

2. Picosecond time-resolved fluorescence measurements have revealed a decrease in the relative yield of fluorescence in the nanosecond time regimen (time constant of 5.5 ns) (Delaney et al., 1993). These fluorescence data indicate that the relaxation properties of the excited electronic state populated by excitation of K-590 changes (perhaps via altered retinal-protein interactions) within the nanosecond interval preceding the formation of L-550 (Delaney et al., 1993).

3. The presence of an intermediate that is vibrationally distinct from both K-590 and L-550 at RT, as well as from K-610 at LT, has been derived from IR absorption spectra recorded at LT, where specific BR species are thermally stabilized (Rothschild et al., 1985; Sasaki et al., 1993). The vibrational spectrum of the K-610 species trapped at 77K has been measured (e.g., Braiman and Mathies, 1982; Rothschild and Marrero, 1982; Siebert and Mäntele, 1983). The mixture of BR photoproducts trapped at 135K contains both K-610 and a second K-like, red-shifted species. The two K species have been distinguished via the different illumination conditions that drive their respective back-reactions to reform BR-570 (Rothschild et al., 1985; Sasaki et al., 1993). In addition, the specific bands appearing in the 980-cm^{-1} to 990-cm^{-1} range differ between the two K species at RT.

4. Time-resolved vibrational spectra assignable to K-590 at RT have been measured with picosecond time resolution (Hsieh et al., 1981, 1983; Stern and Mathies, 1985; Brack and Atkinson, 1989; Doig et al., 1991; Diller et al., 1991, 1992; Atkinson and Ujj, 1992; Lohrmann et al., 1995; Althaus et al., 1995; Ujj et al., 1996). Recently, picosecond time-resolved coherent anti-Stokes Raman spectra (PTR/CARS) from both native K-590 at RT and an isotopically labeled ($^{13}C_{14,15}$) K-590 at RT have been reported (Ujj et al., 1996; Jäger et al., 1996).

Time-resolved RR spectra from K-590 at RT contain different HOOP bands. For example, the HOOP bands found in the 13.7 ns data (Doig et al., 1991) do not appear in the 6 ps data (Doig et al., 1991). An independent change appears as a 3-cm^{-1} shift of the band assigned to the C=C stretching mode (Doig et al., 1991). These differences have been associated with the transformation between ps/K-590 and KL (ns/K-590) and used to derive a 70-ps rise time for KL (Doig et al., 1991).

Time-resolved vibrational RR (Terner et al., 1979; Hsieh et al., 1981, 1983; Smith et al., 1983; Braiman and Mathies, 1983; Braiman, 1986; Lohrmann et al., 1991, 1995; Lohrmann and Stockburger, 1992; Althaus et al., 1995) and IR (Nölker et al., 1992; Sasaki et al., 1993, 1995; Weidlich and Siebert, 1993; Hage et al. 1996) spectra from K-590 at RT have been measured with submicrosecond time resolution. These spectra also have been utilized to identify different K-590 species via the appearance of a new band at 984 cm^{-1} in the nanosecond time regime. The 984-cm^{-1} band has been associated with the ps/K-590 to KL (ns/K-590) transformation (Lohrmann et al., 1991, 1995; Lohrmann and Stockburger, 1992; Nölker et al., 1992; Sasaki et al., 1993, 1995; Weidlich and Siebert, 1993; Althaus et al., 1995; Hage et al., 1996). Specifically, comparisons of RR spectra recorded at 10 ps, 6 ns, and 2 μs suggest the appearance of a species within the 50-ns to 250-ns interval (Lohrmann et al., 1995; Althaus et al., 1995). The comparison of IR bands measured between 900 cm^{-1} and 1400 cm^{-1} and with time delays between −120 ns and 860 ns (instrumental response time of 60 ns) give a rise time of ~10 ns (Sasaki et al., 1995). A small intensity decrease of the 958-cm^{-1} band also has been attributed to the appearance of KL (Sasaki et al., 1995). A recent time-resolved FTIR study presents spectra taken in the 20-ns to 940-ns time range after laser excitation that have been described as corresponding to a mixture of K-590 and KL (Hage et al., 1996).

The time-resolved spectrum of L-550 at RT has been measured in several studies using different RR methods (e.g., Stockburger et al., 1986; Ames and Mathies, 1990) and infrared techniques (e.g. Braiman et al., 1991; Uhmann et al., 1991; Hessling et al., 1993).

Despite the attention given to K-590, a precise determination of the vibrational changes in K-590 at RT over the 10-ps to 1-μs time regimen has remained difficult to establish, because to do so involves the accurate, quantitative measurements of small differences between time-resolved vibrational spectra. The signal-to-noise (S/N) ratio found in time-resolved RR and IR data reported to date has not been sufficiently high to quantitatively compare vibrational spectra from separate BR intermediates recorded at different

delay times in the 10-ps to 260-ns time regime. The PTR/CARS data reported here provide a unique opportunity to obtain such high S/N vibrational data as evidenced from recently published data from intermediates in the BR and rhodopsin photoreactions at RT (Ujj et al., 1996; Jäger et al., 1996; Popp et al., 1996). Highly reproducible (<3% error functions) PTR/CARS spectra are obtained with accumulation times of <300 s. It is also important to note that excitation of the RT/BR photocycle in PTR/CARS experiments is achieved with a <3-ps pulse, which minimizes any secondary photochemistry and/or back-reactions that can significantly confuse the chemical reaction being investigated.

In this paper, PTR/CARS vibrational spectra over the 750-cm^{-1} to 1720-cm^{-1} range are reported for the 50-ps to 260-ns time regime of the RT/BR photocycle. Although most of the vibrational bands assigned to K-590 at RT remain unchanged for the 50-ps to 260-ns time range, a new vibrational band of significant intensity appears at 984 cm^{-1}, and at least nine other bands substantially change either in position or intensity or both. Of these latter changes in vibrational features, there are two types: those observable directly from the PTR/CARS data recorded at different times (Figs. 1 and 2) and those small enough to be observable only in the quantitative subtraction of PTR/CARS that are plotted as Δ(PTR/CARS) (Figs. 4 and 5). In all nine cases, these differences are significantly above the measurement noise as determined by repetitive experiments. Based on previous vibrational mode assignments of these bands in both time-resolved (Ujj et al., 1996; Jäger et al., 1996; Weidlich and Siebert, 1993) and LT vibrational (Smith, 1985; Maeda et al., 1991) spectra, it is evident that the retinal structure near the C_{14}-C_{15}=N bonds (Schiff-base region) and along its polyene chain is altered during the 50-ps to 260-ns interval. These spectral changes may also reflect alterations in the protein adjacent to the Schiff base linkage. The time constant of the changes is estimated to be 40–70 ns.

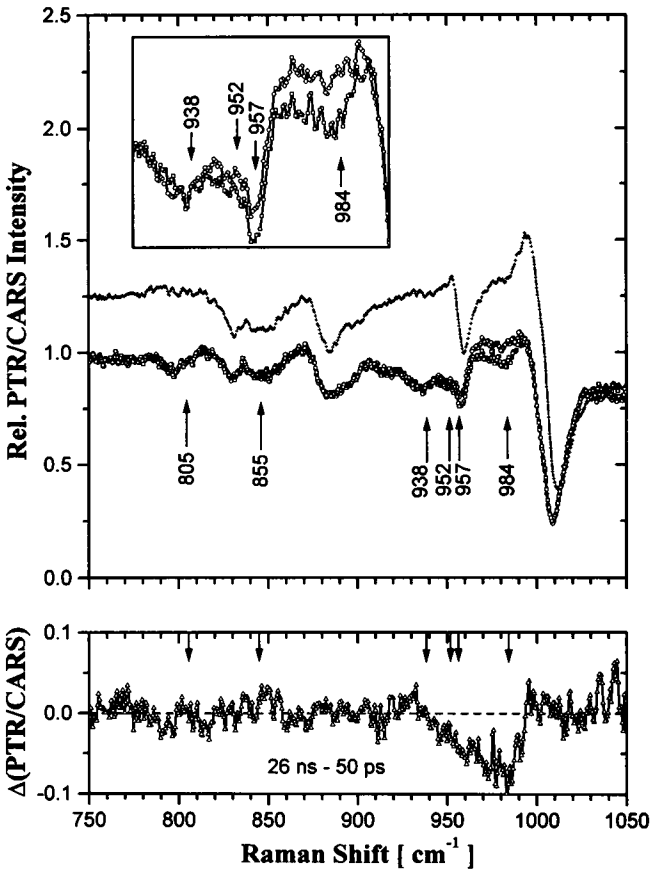

FIGURE 1 PR/CARS spectrum of BR-570 (+) and PTR/CARS spectra of the reactive mixture comprising BR-570 and K-590, recorded with time delays of 50 ps (○) and 26 ns (□) for the 750 cm^{-1} to 1050 cm^{-1} region (HOOP region). An offset of 0.5 is added to the vertical scale of the PR/CARS spectrum to facilitate comparisons. Vertical arrows mark six differences between the spectra of 50 ps and 26 ns. Four of these differences are highlighted in the inset, which has an expanded vertical scale. Differences between two spectra (26 ns minus 50 ps) are shown as Δ(PTR/CARS) at the bottom (△).

EXPERIMENTAL

A detailed description of the experimental setup and of the theoretical background for the PTR/CARS measurements is described elsewhere (Ujj et al., 1994a,b, 1996; Jäger et al., 1996). Only the actual measuring conditions used and the basics of the data analysis are described here.

MATERIALS AND METHODS

BR is grown from a cell line of *Halobacterium salinarium* and purified according to established procedures (Oesterhelt and Stoeckenius, 1974).

Instrumentation

Three dye lasers (Coherent, model 700), operating at 400-kHZ repetition rates with separate cavity dumpers (Coherent, models 7210 and 7220), are synchronously pumped by the second-harmonic output (527 nm) of a mode-locked Nd:YLF laser (Coherent, Antares 76 YLF). PTR/CARS data are recorded by using the pump (ω_p) laser pulses to excite BR-570 and, thereby, to initiate the BR photocycle. The two probe (ω_l and ω_s) laser pulses generate CARS signals at variable time delays (between 50 ps and 260 ns) from the BR-570/K-590 mixture. The experimental parameters describing the lasers pulses are 1) ω_p: 570 nm, 0.7 mW/1.75 nJ/pulse, 3 ps (FWHM), bandwidth ≈ 50 cm^{-1}; 2) ω_l: 665 nm, 0.5 mW/1.25 nJ/pulse, 7 ps (FWHM), bandwidth < 4 cm^{-1}; and 3) ω_s: 720 nm, 1.35 mW/3.38 nJ/pulse, 7 ps (FWHM), bandwidth ≈ 350 cm^{-1}.

The independently controlled optical delay lines are used to determine the timing sequence between the ω_p, ω_l, and ω_s laser pulses over the 50-ps to 1-ns regime. Electronic synchronization of the three separate cavity dumpers utilized with the three dye lasers controls the pulse sequencing in the 1–260-ns interval (via steps of 13 ns).

A reservoir of 15–20 ml of BR sample ($OD_{Samples}$ at 570 nm ≈ 4/cm) is constantly illuminated with the output from a halogen lamp to ensure complete light adaptation throughout the entire PTR/CARS measurement. The sample is kept at a temperature of 17°C. BR is examined as a flowing fluid jet that is pumped with a laminar speed of 15 m/s through a glass nozzle (400-mm diameter). The laser beams are focused within the sample jet on an area with a diameter of 20 μm. The flow rate and focusing conditions ensure that the laser pulses always encounter a new sample volume.

The PTR/CARS signals are detected with a triple monochromator and a reticon multichannel array detector (EG&G/PARC, model 1420).

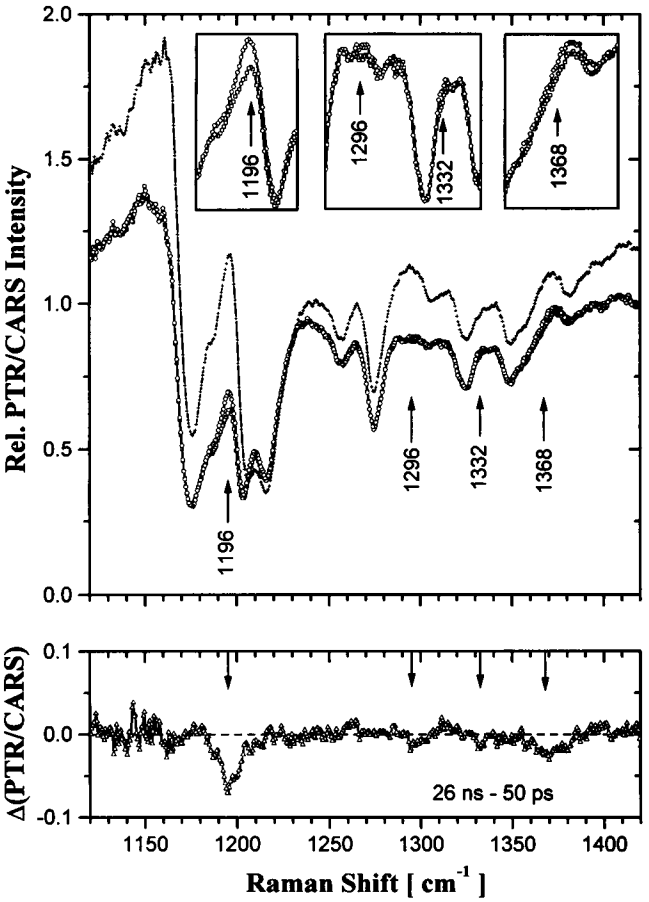

FIGURE 2 PR/CARS spectrum of BR-570 (+) and PTR/CARS spectra of the reactive mixture comprising BR-570 and K-590, recorded with time delays of 50 ps (○) and 26 ns (□) for the 1020 cm^{-1} to 1420 cm^{-1} region (C-C stretching region). An offset of 0.5 is added to the vertical scale of the PR/CARS spectrum to facilitate comparisons. Vertical arrows mark four differences between the spectra of 50 ps and 26 ns. The differences are highlighted in the insets, which have expanded vertical scales. Differences between two spectra (26 ns minus 50 ps) are shown as Δ(PTR/CARS) at the bottom (△).

Before each PTR/CARS measurement, the degree of excitation in BR-570, and thereby the relative concentration of K-590 in the flowing sample, is measured using picosecond transient absorption (PTA). These PTA data are collected using the same optical and sample configuration as that used in the PTR/CARS measurements. PTA data demonstrate that 15–20% of the BR-570 is optically excited, and the degree of optical perturbation of BR-570 caused by the two probe pulses is <1%.

The pumping and probing conditions are selected to minimize secondary excitation of photocycle intermediates and thereby to minimize back-reactions and irreversible side-reactions that could alter either the spectra or kinetics of the BR photocycle (Delaney et al., 1993; Yamamoto et al., 1994). This phenomenon is extensively discussed earlier (Ujj et al., 1996).

At longer time delays (>100 ns), the potential for spatial mismatch of the ω_p, ω_l, and ω_S beams within the flowing BR sample is considered. Because the PTR/CARS and PTA measurements rely on exciting and probing the same sample volume, any spatial mismatch would introduce an erroneous change in spectral signals. The potential decrease in the K-590 concentration due to a spatial mismatch can be estimated assuming a Gaussian intensity profile of pump and probing beams, each having a spatial dimension (HWHM) of 10 μm and a sample flow speed of 15 m/s. An additional decrease in the amount of K-590 is associated with its decay to L-550 (life-time ≈ 1 μs at RT; e.g., Váró and Lanyi, 1991; Lohrmann and Stockburger, 1992; Sasaki et al., 1993). This effect accounts for decreases in the K-590 concentration of about 3%, 13%, and 23% at delays of 26 ns, 130 ns, and 260 ns, respectively. Considering these values the PTA signals monitoring the concentration of K-590 at 50 ps, 26 ns, 130 ns, and 260 ns are used to align the pumping laser beam relative to the two probing beams so as to minimize any spatial effect. Experimental errors in beam alignment could maximally alter the K-590 concentration by <10%.

Procedurally, the spectrum of the reference water sample (i.e., the nonresonant background CARS signal) is measured first. The water sample is replaced by the light-adapted BR sample, and the PR/CARS spectrum of BR-570 is recorded. Subsequently, the PTR/CARS data at different time delays are measured in the order 50 ps, 1 ns, 13 ns, 260 ns, 50 ps, 26 ns, 130 ns, and 260 ns. Data taken at 50 ps and 260 ns are collected twice to determine the stability of the system (repetitive BR-570 and water sample data are also compared). To obtain PTR/CARS spectra with sufficient S/N, a 30-s accumulation time is typically used and repeated 10 times. The entire series of time-delay measurements is completed in 90 min.

Theoretical

PTR/CARS data are quantitatively analyzed by third-order susceptibility $\chi^{(3)}$ relationships. The $\chi^{(3)}$ function describing a BR sample is related directly to the electronic and vibrational properties of its chromophoric species (i.e., retinal). The $\chi^{(3)}$ analysis provides amplitudes, bandwidths, and band origin positions of all vibrations that undergo the coherent resonant anti-Stokes Raman scattering. It includes a fitting procedure of the data that utilizes a model function derived for a sample containing a mixture of chromophoric BR species (Ujj et al., 1994a,b). The theoretical background for the case of a sample containing BR-570 and a transient concentration of K-590 has been described previously (Ujj et al., 1996). Because structurally distinct K-590 species have the same visible absorption maximum (Delaney et al., 1993; Yamamoto et al., 1994), only two phase factors, one for BR-570 and one for K-590 (Ujj et al., 1996), are included in the fitting procedure.

Each PTR/CARS spectrum is normalized to the water reference signal. Differences between two corrected PTR/CARS spectra, recorded at different time delays, define the Δ(PTR/CARS) signals appearing in the figures. Δ(PTR/CARS) spectra (e.g., 1 ns minus 50 ps, 13 ns minus 50 ps, 26 ns minus 50 ps, 130 ns minus 50 ps, and 260 ns minus 50 ps) reveal structural changes during the transient lifetime of K-590. Theoretically, a Δ(PTR/CARS) spectrum from a mixture of different species (e.g., BR-570, ps/K-590, ns/K-590) results in a complex signal. Thus a qualitative analysis of Δ(PTR/CARS) spectra can only identify which features have changed, but can neither eliminate the involvement of other bands (e.g., bands are strongly overlapping) nor distinguish between changes of intensities and/or band positions. Quantitative $\chi^{(3)}$ fits to each PTR/CARS spectrum are made 1) to characterize which additional bands have changed as a function of delay time and 2) to determine whether band positions, relative intensities, or both have changed. The $\chi^{(3)}$ analysis specifies the changes of the band parameters for different species of K-590 within the error limit of the fitting procedure (<5%).

RESULTS

PR/CARS spectra from BR-570 alone (probe only data) for three spectral regions, 750-1050 cm^{-1} (hydrogen-out-of-plane, HOOP), 1120–1420 cm^{-1} (C-C stretching), and 1420–1720 cm^{-1} (C=C stretching/C=NH^+ stretching), are presented in Figs. 1–3. PTR/CARS data from K-590, recorded with 50-ps and 26-ns delays, are also presented in Figs. 1–3 for these respective spectral regions.

The differences between the two PTR/CARS spectra, recorded at different delays (i.e., 26 ns minus 50 ps), are shown as Δ(PTR/CARS) and presented on an expanded

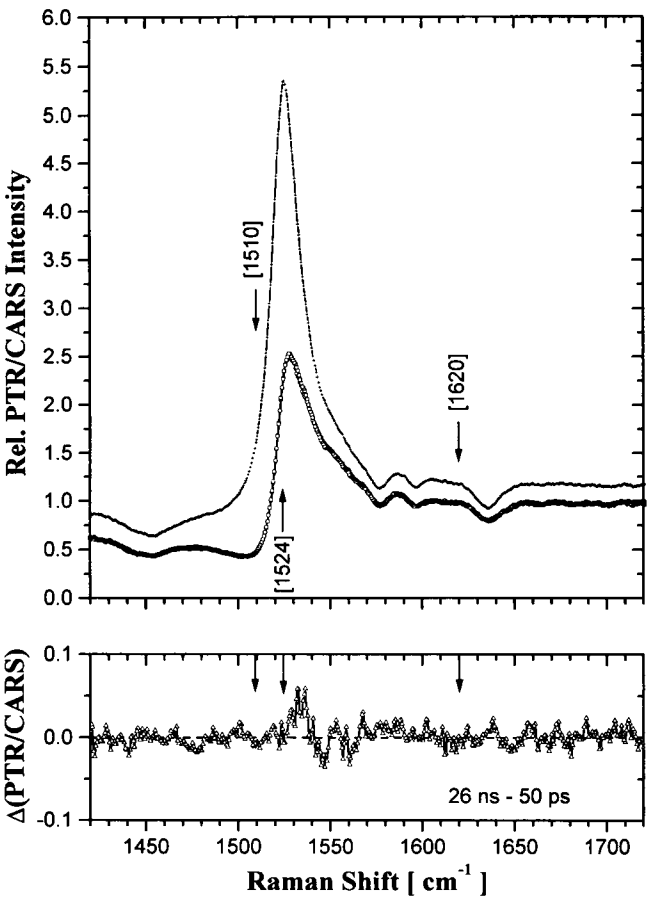

FIGURE 3 PR/CARS spectrum of BR-570 (+) and PTR/CARS spectra of the reactive mixture comprising BR-570 and K-590, recorded with time delays of 50 ps (○) and 26 ns (□) for the 1420 cm^{-1} to 1720 cm^{-1} region (C=C stretching and Schiff-base region). An offset of 0.5 is added to the vertical scale of the PR/CARS spectrum to facilitate comparisons. No significant differences are observed between the spectra of 50 ps and 26 ns. Vertical arrows together with respective band positions in brackets mark the positions of major C=C stretching modes (1510 cm^{-1} and 1524 cm^{-1}) and the position of the $C{=}NH^{+}$ mode of the Schiff base (1620 cm^{-1}), as reported from recent RR studies. Differences between two spectra (26 ns minus 50 ps) are shown as Δ(PTR/CARS) at the bottom (△).

intensity scale at the bottom of each of these figures. Most of the vibrational features in the 50-ps and 26-ns spectra are the same, thereby indicating that major parts of the retinal structure have not been altered over this time interval. Distinct differences do appear, however, in the vibrational spectrum of K-590 as the BR photocycle evolves from 50 ps to 26 ns.

Hydrogen-out-of-plane (HOOP) region

The main 50-ps/26-ns change in the HOOP region occurs at 984 cm^{-1}, where a new band appears (Fig. 1). Other changes, between 935 cm^{-1} and 960 cm^{-1}, are highlighted in the insets shown in Fig. 1. The time-dependent intensity increase of the band at 984 cm^{-1} is measured in the Δ(PTR/CARS) data obtained by subtracting the spectrum of 50 ps from those recorded at 1 ns, 26 ns, 130 ns, and 260 ns, respectively (Fig. 4). These Δ(PTR/CARS) spectra also reveal the changes in the 935–960-cm^{-1} region, as well as small features near 805 cm^{-1} and 855 cm^{-1}.

C-C stretching region

A change in the 1196-cm^{-1} band occurring between 50 ps and 26 ns (Fig. 2) becomes unambiguous when the intensity scale of the Δ(PTR/CARS) spectrum is expanded by a factor of 7 and the time-dependence scale is extended to 130 ns (Fig. 5). In separate experiments, the Δ(PTR/CARS) spectrum is obtained by subtracting the 50-ps PTR/CARS spectrum from 26-ns PTR/CARS data (Fig. 5). The same change in the 1196-cm^{-1} band (relative to the 50 ps data) is found at 26 ns (Fig. 5). The insets in Fig. 2, as well as the three Δ(PTR/CARS) spectra (Fig. 5), establish the presence of small intensity and wavelength changes around the 1296 cm^{-1}, 1332 cm^{-1}, and 1368 cm^{-1} bands.

C=C stretching and Schiff base region

It is especially revealing to note that the K-590 vibrational spectra exhibit no significant changes in the 1420–1720-

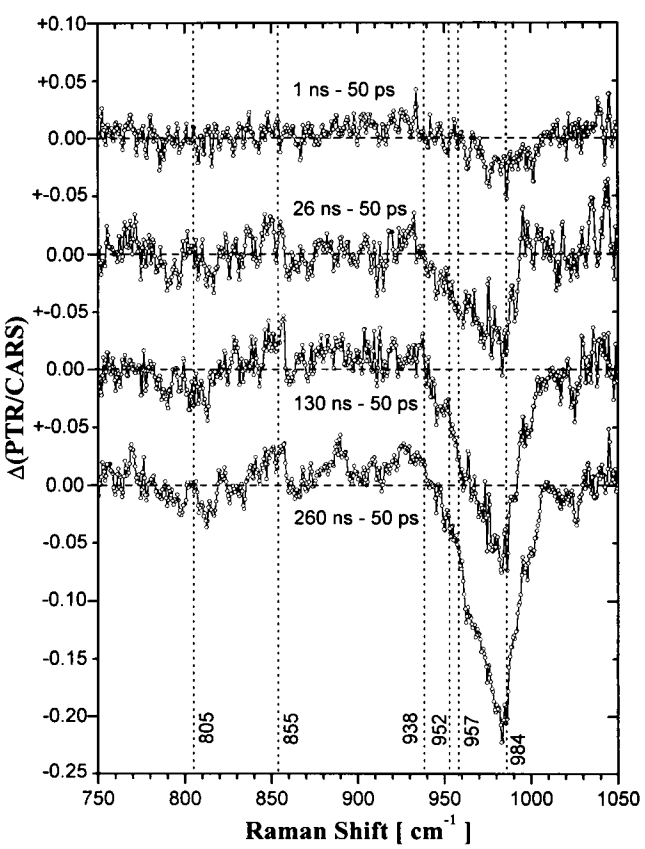

FIGURE 4 Difference spectra, Δ(PTR/CARS), recorded at different time delays (i.e., 1 ns minus 50 ps, 26 ns minus 50 ps, 130 ns minus 50 ps, and 260 ns minus 50 ps). The time-dependent increase of the band at 984 cm^{-1} is observed. Other changes occur in at least five additional spectral regions and are marked by dotted vertical lines.

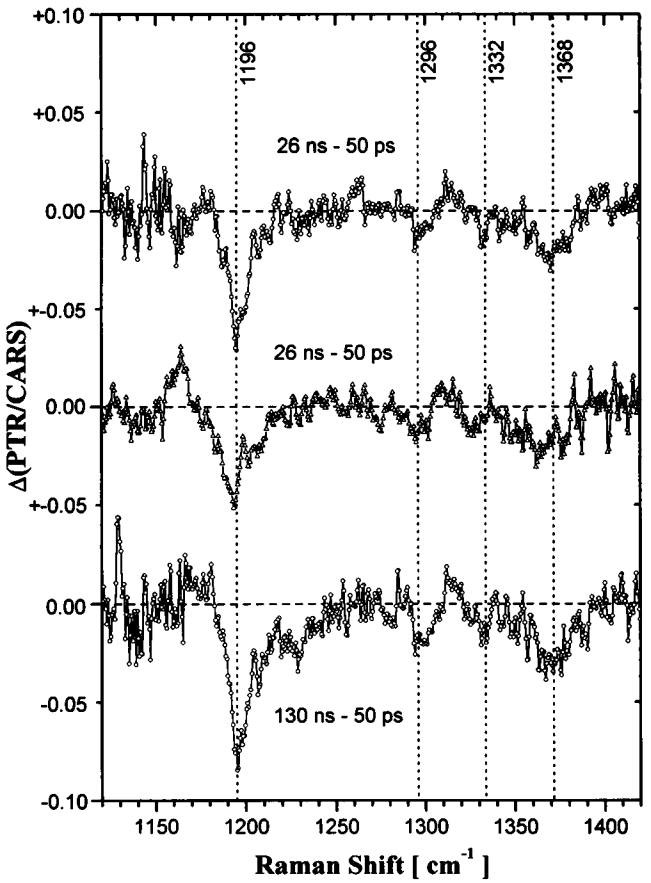

FIGURE 5 Difference spectra, Δ(PTR/CARS), recorded at different time delays (i.e., 26 ns minus 50 ps, and 130 ns minus 50 ps). Each Δ(PTR/CARS) spectrum is obtained in a separate experiment. The main change occurs at 1196 cm^{-1}, but smaller changes occur in at least three additional spectral regions. The changes are marked by dotted, vertical lines. The excellent reproducibility of these PTR/CARS data is established in the results of the two repetitive experiments (26 ns minus 50 ps) shown here.

cm^{-1} region over time delays of 50 ps to 26 ns. Not only does the major C═C stretching band at 1524 cm^{-1} remain unchanged, but no band(s) assignable to the C═NH^+ mode is found (located between 1600 cm^{-1} and 1640 cm^{-1}, as reported from LT/RR (e.g., Braiman and Mathies, 1982) and RT/RR studies in the nanosecond time regime (e.g., Stern and Mathies, 1985; Lohrmann et al., 1991)). Expansion of the intensity scale used to display the 50-ps/26-ns Δ(PTR/CARS) spectrum indicates that no changes (within a factor of 2; S/N ≈ 35) can reasonably be detected.

Contributions to PTR/CARS spectra from vibrational bands assignable to the L-550 intermediate also can be considered. Given the 1-μs time constant for the K-590 to L-550 transformation (e.g., Váró and Lanyi, 1991), <3%, <13%, or <23% of the total transient mixture of species present in the BR photocycle examined at the delay of 26 ns, 130 ns, or 260 ns, respectively, can be attributed to L-550. The blue-shifted (relative to that of K-590) L-550 absorption maximum is far from resonance with the λ_l (665 nm) and λ_a (~615 nm) wavelengths used to measure the PTR/CARS signal, and therefore the resonance enhancement effect associated with L-550 Raman scattering is minimal. Indeed, no indications of any CARS signal, even from the strong C═C stretching features in the 1535–1555 cm^{-1} region (e.g., Stockburger et al., 1986; Ames and Mathies, 1990) assigned to L-550, are found in the PTR/CARS spectra described here. The concentration change in K-590 due to its decay to L-550 is approximately the same as the S/N ratio (~50 in the C═C stretching region) in the spectrum taken at 26 ns (<3%) and, therefore, is negligible. Time-dependent changes in the K-590 concentration can be observed, however, in PTR/CARS spectra, especially at 1510 cm^{-1} and 1524 cm^{-1}, where the intense ethylenic modes of K-590 are located (Ujj et al., 1996).

The time-dependent evolution of the K-590 vibrational spectrum between 50 ps and 26 ns indicates that changes in the vibrational structure of the retinal chromophore are occurring. *No such spectral changes arise in the picosecond time regime.*

A quantitative analysis of the $\chi^{(3)}$ fit to the PTR/CARS data can elucidate more specific changes. As shown in previous PTR/CARS studies of BR (Ujj et al., 1994a,b), the function describing the error between the $\chi^{(3)}$ fits and the PTR/CARS data is <3–5%. The PTR/CARS spectrum recorded at 50 ps (this study) contains all of the bands recently reported and assigned to ps/K-590 at RT (Ujj et al., 1996). Deviations in band positions are <2 cm^{-1} and variations in relative amplitudes are found to be 30% at most. The largest errors are found for strongly overlapping bands (near 950 cm^{-1}, 1190 cm^{-1}, and 1520 cm^{-1}) and for low-intensity bands (S/N < 4). Recently, unambiguous $\chi^{(3)}$ fit parameters have been calculated by taking into account spectra of ps/K-590 measured for at least five different BR-570 concentrations (Ujj et al., 1996). To obtain high S/N, the PTR/CARS data reported here are recorded at high concentrations of the sample (OD_{Sample}(568 nm) ≈ 4/cm). At high concentrations, the calculated band parameters of the $\chi^{(3)}$ fit could be different compared to the exact values. Changes of this type can be attributed to the nonhomogeneous spatial population distribution over the diameter of the sample nozzle as created by the excitation beam (400 μm). These changes do not effect the conclusions presented here.

Comparisons of the PTR/CARS data with previously published time-resolved RR spectra assigned to K-590 are facilitated if the nonresonant background contribution is quantitatively removed from the PTR/CARS data and the vibrational bands are given as Lorentzian lineshapes (RR spectra are described by band intensities, whereas CARS spectra with Lorentzian lineshapes are described by band amplitudes). The methodology for quantitatively representing the nonresonant background contribution in PTR/CARS spectra from BR is described elsewhere (Ujj et al., 1994b), as has been the rationale supporting the use of Lorentzian lineshapes (Ujj et al., 1996).

PTR/CARS data from ps/K-590 (Ujj et al., 1996) without the nonresonant background contain band positions with error < 1 cm^{-1} (Fig. 6). The 50-ps/26-ns Δ(PTR/CARS)

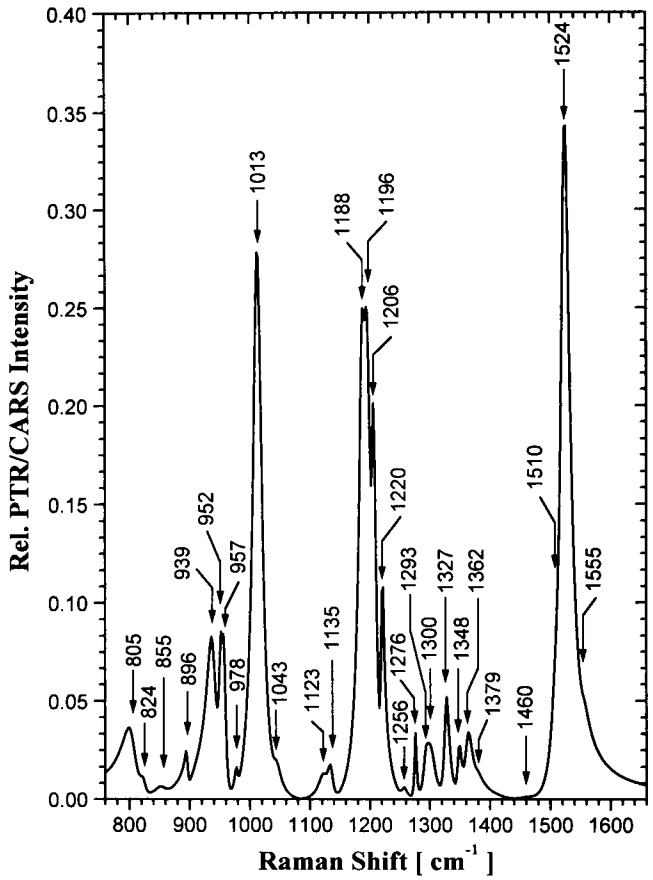

FIGURE 6 A $\chi^{(3)}$ fit to the PTR/CARS spectrum without nonresonant backgrounds and utilizing Lorentzian lineshapes of ps/K-590 for the 760 cm^{-1} to 1670 cm^{-1} region. The origin positions of the vibrational bands are indicated. The PTR/CARS spectrum of K-590 is taken from Ujj et al. (1996).

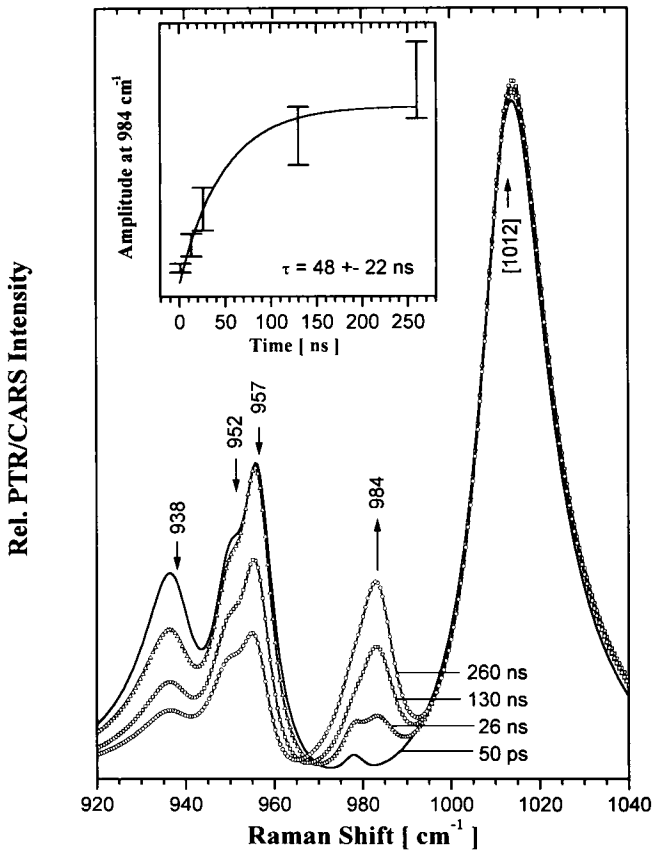

FIGURE 7 The $\chi^{(3)}$ fits to the PTR/CARS spectra without nonresonant backgrounds and utilizing Lorentzian lineshapes of K-590 for the 920 cm^{-1} to 1040 cm^{-1} region, as measured at four different time delays: 50 ps (−), 26 ns (△), 130 ns (□), and 260 ns (○). An intensity increase of the new band at 984 cm^{-1} and an intensity decrease of the bands at 938 cm^{-1}, 952 cm^{-1}, and 957 cm^{-1} are observed. The intensity of the methyl rocking vibrations at 1012 cm^{-1} is not changing significantly (<5%). The inset displays the amplitude increase of the band at 984 cm^{-1} at different time delays, which is described by a single exponential, time constant of 48 ± 22 ns.

spectra (Figs. 1–5) reveal small intensity and/or position changes for the bands at 805 cm^{-1} and 855 cm^{-1} in the HOOP region and at 1300 cm^{-1}, 1327 cm^{-1}, and 1362 cm^{-1} in the C-C stretching region. Because the features around 1296 cm^{-1} and 1368 cm^{-1} (Fig. 5) are broad, additional changes at 1293 cm^{-1} and 1379 cm^{-1} cannot be excluded. These small intensity changes are not quantitatively measured in the $\chi^{(3)}$ fits, because they are on the order of the errors in the fit itself (<5%). In comparison with the $\chi^{(3)}$ fit parameters found for the spectrum at 50 ps in the C-C stretching region, the 26-ns spectrum can be suitably fit only by increasing the amplitude of the 1196 cm^{-1} by 13% and increasing its frequency by <1 cm^{-1} (data not shown). Changes in the fit parameters for the bands at 1188 cm^{-1} and 1206 cm^{-1} have not been considered because of the ambiguities in their respective fits.

PTR/CARS spectra without the nonresonant background, over the HOOP region (920 cm^{-1} and 1040 cm^{-1}), are shown in Fig. 7 for four different time delays. Sequentially, measurements are recorded at 50 ps, 1 ns, 13 ns, 260 ns, 50 ps, 26 ns, 130 ns, and 260 ns, with the data from 50 ps and 260 ns collected twice to determine reproducibility. These spectra establish the intensity increase of a new band at 984 cm^{-1} and the intensity decrease in the bands at 938 cm^{-1}, 952 cm^{-1}, and 957 cm^{-1}. Obviously the latter bands do not decay completely. The intensity of the methyl rocking vibrations at 1012 cm^{-1} is not changing significantly (<5%).

The time constant describing the intensity increase of the 984-cm^{-1} band can be estimated (Fig. 7, *inset*) if its relative intensity at different time delays is normalized relative to the K-590 concentration (i.e., the 1-μs transformation from K-590 to L-550 (e.g., Váró and Lanyi, 1991) is considered). The intensity errors for the 1 ns, 13 ns, and 26 ns data are derived from the <30% error in the intensities of the weaker bands. A <20% intensity error is used for the 130 ns and 260 ns data, whereas <10% is used for the most intense bands (S/N > 4). An additional 10% is used to reflect the uncertainty in the alignment of the pump and probing beams (see Experimental). For a single exponential fit with a constant offset of zero, the weighted fit gives a life-time of 48 ± 22 ns (Fig. 7).

In a similar way, the time constant describing the intensity decrease in the bands at 938 cm^{-1}, 952 cm^{-1}, and 957 cm^{-1} is derived. Because they are strongly overlapping, the relative intensities of these bands can be determined only to within ~30%. Again, an additional 10% error is included to reflect the uncertainty in the alignment of the pump and probing beams for 130-ns and 260-ns delays. The single exponential decay fit (not shown), including an offset, is 30–170 ns (938 cm^{-1}), 40–120 ns (952 cm^{-1}), and 40–300 ns (957 cm^{-1}), respectively.

DISCUSSION

The PTR/CARS results presented here demonstrate that a few selected changes in the vibrational spectrum of K-590 occur between 50 ps and 260 ns and that two structurally distinct K-590 species are present during the 50-ps to 260-ns interval in the RT/BR photocycle.

The most pronounced change is the appearance of a new band at 984 cm^{-1}. The result is consistent with time-resolved vibrational studies reported earlier that show that the 984-cm^{-1} band appears in the nanosecond time regime: RR data (Terner et al., 1979; Hsieh et al., 1981, 1983; Smith et al., 1983; Braiman and Mathies, 1983; Braiman, 1986; Doig et al., 1991; Lohrmann et al., 1991, 1995; Lohrmann and Stockburger, 1992; Althaus et al., 1995) and IR absorption data (Nölker et al., 1992; Sasaki et al., 1993, 1995; Weidlich and Siebert, 1993; Hage et al., 1996).

The nanosecond K-590 (ns/K-590) species is vibrationally distinct from picosecond K-590 (ps/K-590). The ns/K-590 species may be the same as that previously termed KL (e.g., Sasaki et al., 1993; Weidlich and Siebert, 1993; Lohrmann et al., 1995; Hage et al., 1996). Based on results from earlier studies, the visible absorption changes used to propose the existence of KL (Shichida et al., 1983; Milder and Kliger, 1988) could not be reproduced when lower energy, picosecond pulsed excitation is used to measure transient absorption (Delaney et al., 1993; Yamamoto et al., 1994). To more precisely denote the structural differences reflected in the vibrational spectroscopy, the species described in this work is termed ns/K-590, and not KL. The ps/K-590 to ns/K-590 transformation emphasizes the similarity to the K-590 species present in the 50-ps to 260-ns time regime, while still noting the significant structural differences.

Assignment of the vibrational changes

The interpretation of the vibrational changes between ps/K-590 and ns/K-590, as monitored by PTR/CARS, depends directly on the modes to which these specific vibrational features are assigned. Vibrational mode assignments are taken from several sources, including LT/RR and LT/FTIR data of thermally stabilized BR (Smith, 1985; Maeda et al., 1991), as well as time-resolved CARS (Ujj et al., 1996; Jäger et al., 1996) and FTIR data (Weidlich and Siebert, 1993) from RT/BR.

Hydrogen-out-of-plane region

805-cm^{-1} band

The 805-cm^{-1} band shifts to a lower frequency upon deuteration of the Schiff base nitrogen (Ujj et al., 1996). The band corresponds to the 812-cm^{-1} band observed in LT/RR spectra of K-610 that has been identified as containing the C_{14}-HOOP vibration (Smith, 1985).

855-cm^{-1} band

The frequency of the 855-cm^{-1} band decreases in D_2O (Ujj et al., 1996). LT/RR data contain a band at 868 cm^{-1}, which has been assigned to the C_{11}-C_{12}-HOOP vibrational mode (Smith, 1985).

938-cm^{-1} band

The frequency of the 938-cm^{-1} band is clearly sensitive to the deuteration of the Schiff base nitrogen (Ujj et al., 1996). At LT, a band at 943-cm^{-1} band appears that is sensitive to C=NH/D deuteration and is assigned to the C_{11}-C_{12}-HOOP vibrational mode.

952-cm^{-1} band

The 952-cm^{-1} band shifts to lower frequency upon deuteration of the Schiff base nitrogen (Ujj et al., 1996). This band is not resolved in LT studies and has not yet been assigned to a vibrational mode.

957-cm^{-1} band

The 957-cm^{-1} band has been assigned to the C_{15}-HOOP mode of K-610 at LT (Smith, 1985; Maeda et al., 1991). This band does not exhibit a temperature dependence because it appears at the same position in PTR/CARS data recorded from K-590 at RT and the LT/RR spectrum of K-610 (Smith, 1985). It does, however, exhibit a clear sensitivity to deuteration at the Schiff base nitrogen in the RT/BR photocycle, as observed in the PTR/CARS data from K-590 (Ujj et al., 1996).

984-cm^{-1} band

Based on time-resolved FTIR measurements (Weidlich and Siebert, 1993), the 984-cm^{-1} band is also assigned to the C_{15}-HOOP mode that is coupled to the NH-HOOP mode.

C-C stretching region (fingerprint)

1196-cm^{-1} band

The 1196-cm^{-1} band is the strongest in the fingerprint region (compared to the bands at 1188 cm^{-1}, 1206 cm^{-1}, and 1220 cm^{-1}). These bands are all assigned to highly mixed vibrations of C-C stretching modes (Jäger et al., 1996). The 1196-cm^{-1} band contains significant C_{14}-C_{15} stretching character (Jäger et al., 1996), as well as some hydrogen-in-plane rocking character (Smith, 1985).

1300-cm^{-1} band

This low-intensity band at 1300 cm^{-1} is not sensitive to deuteration of the Schiff base nitrogen (Ujj et al., 1996). The stronger 1293-cm^{-1} band located nearby does shift substantially to lower frequency upon deuteration (Ujj et al., 1996). The 1300-cm^{-1} band probably corresponds to the 1295-cm^{-1} band observed in LT/RR spectra that has been assigned to C_{10}-H and C_{11}-H in-plane rocking vibration (Smith, 1985).

1327-cm^{-1} band

The low-intensity 1327-cm^{-1} band is only slightly sensitive to deuteration of the Schiff base nitrogen (Ujj et al., 1996). It appears at the same position in LT data and has been assigned to the C_7-H in-plane rocking vibration (Smith, 1985).

1362-cm^{-1} band

The 1362-cm^{-1} band is sensitive to deuteration of the Schiff base nitrogen (Ujj et al., 1996). The nearby weak band at 1379 cm^{-1} also shifts upon deuteration (Ujj et al., 1996).

The vibrational modes that change during the ps/K-590 to ns/K-590 transition directly reflect structural alterations in retinal chromophore. Their vibrational mode assignments provide a detailed view of changes in the retinal structure occurring over the 50-ps to 260-ns interval of the RT/BR photocycle. Independently, some understanding of the chromophore-protein interaction after all-*trans* to 13-*cis* isomerization also can be obtained.

Comparisons with previous vibrational data

Several results from these PTR/CARS data are at variance with previously published data:

1. The K-590 PTR/CARS spectra recorded at 50 ps and 1 ns do not contain bands near 990 cm^{-1}, as previously reported for time delays between 200 ps and 20 ns (Stern and Mathies, 1985).

Analogous HOOP features have been found in the 50-ps to 2-ns interval (Brack and Atkinson, 1989). The assignment of these features near 990 cm^{-1} may involve vibrationally excited species because the probing powers used in these RR experiments are sufficiently high to create vibrationally excited, ground-state BR-570 (or perhaps K-590) populations. Independently, assignments to vibrational modes in other photoproducts created via secondary photoreaction may also be associated with the 990-cm^{-1} features. These 990-cm^{-1} features are not reported in RR data recorded with lower probing powers (Hsieh et al., 1981, 1983; Lohrmann et al., 1995; Althaus et al., 1995).

2. No band assignable to the C=NH$^+$ stretching vibration at the Schiff base linkage is found in PTR/CARS data recorded from either ps/K-590 or ns/K-590 (Figs. 3 and 6), even though the respective PTR/CARS spectra are measured with excellent S/N (~50). Such a Schiff base mode is reported to appear between 1600 cm^{-1} and 1640 cm^{-1} in the LT/RR measurements of K-610 (Braiman and Mathies, 1982; Rothschild et al., 1985; Smith, 1985; Gerwert and Siebert, 1986).

The effects of high probing power may also be associated with the appearance of the C=NH$^+$ stretching band near 1620 cm^{-1} in RT/RR spectra measured in the picosecond (Stern and Mathies, 1985) and nanosecond time regimes (Terner et al., 1979; Lohrmann et al., 1991, 1995; Lohrmann and Stockburger, 1992; figure 11 in Althaus et al., 1995). Low probe power conditions may ensure that this band appears only as a broad (>10 cm^{-1}), low-intensity (S/N ≈ 2) feature in picosecond (Lohrmann et al., 1995; Althaus et al., 1995) and nanosecond RR data (figure 14 in Althaus et al. 1995). The 1620-cm^{-1} band could not be identified in nanosecond FTIR data obtained under low power conditions (Weidlich and Siebert, 1993). The PTR/CARS data presented here do not rule out the existence of such a small, spectrally broad feature.

3. PTR/CARS data indicate that no changes occur in the ethylenic mode frequencies (1500–1550 cm^{-1}) from 50 ps to 100 ns during the presence of ps/ns K-590 and before the appearance of L-550 (Fig. 3). A 12-cm^{-1} increase in ethylenic frequency, reported from RT/RR data recorded at 200 ps and 20 ns (Stern and Mathies, 1985), is not observed in the PTR/CARS data described here. Differences in probe laser power may underlie the observed frequency shift. The influence of the probe power on the shape and position of bands also has been demonstrated for the ethylenic modes in PTR/CARS data (Atkinson et al., 1994).

By contrast, a 4-cm^{-1} increase in the frequency of the ethylenic mode occurs with a time constant of 40–100 ps (Doig et al., 1991). Analogously, the bandwidth of a broad feature in the HOOP region between 950 cm^{-1} and 1000 cm^{-1} increases with a time constant of 10–40 ps (reported from RR data obtained under low power conditions; Doig et al., 1991). These changes have been attributed to the K-590 to KL transition occurring between 20 and 100 ps (Doig et al., 1991). Possibly the changes arise with a faster time constant than 50 ps. In this case, they could reflect different processes. Intensity changes in vibrational bands within the initial 20 ps of the start of the BR photocycle (i.e., during K-590 formation) have been observed (Stern and Mathies, 1985; Atkinson et al., 1989; Atkinson, 1990; Brack and

Atkinson, 1991; Doig et al., 1991; Diller et al., 1995) and have been interpreted as the J-625 to ps/K-590 transition (Stern and Mathies, 1985; Atkinson et al., 1989; Doig et al., 1991; Diller et al., 1995) and vibrational cooling within the ground state of BR-570 and ps/K-590 (Atkinson, 1990; Brack and Atkinson, 1991; Blanchard et al., 1991).

Rise time of ns/K-590

The time constant describing the transition of ps/K-590 to ns/K-590 can be estimated from the amplitude increase of the band at 984 cm^{-1} and the amplitude decrease of the bands at 938 cm^{-1}, 952 cm^{-1}, and 957 cm^{-1} to be 40–70 ns. This approximation assumes that the same process underlies the changes of all four bands, and that only a single exponential is present. The time constant for the decay of K-590 to L-550 is known to be ~1 μs (e.g., Váró and Lanyi, 1991). A reaction sequence for the BR photocycle (reviewed by Lanyi and Váró, 1995) also contains the back-reaction from L-550 to ns/K-590 (KL) (Váró and Lanyi, 1991; Sasaki et al., 1993; Weidlich and Siebert, 1993). The simplest reaction scheme involving ps/K-590, ns/K-590, and L-550, therefore, can be described:

$$\text{(i) ps/K-590} \Rightarrow \text{ns/K-590} \Leftrightarrow \text{L-550} \ldots$$

No data presented here require the inclusion of a back-reaction from ns/K-590 to ps/K-590 in a sequential scheme or a branching process in the nanosecond time regime that leads to parallel photocycles as well as the presence of different species of BR-570. The existence of parallel photocycles has been proposed previously (Hanamoto et al., 1984; Dáncshazy et al., 1988; Bitting et al., 1990; Birge, 1990; Eisfeld et al., 1993).

The time constants describing the amplitude decrease of the bands at 938 cm^{-1}, 952 cm^{-1}, and 957 cm^{-1} appear to be somewhat longer compared to that of the 984-cm^{-1} band (i.e., 48 $\pm$ 22 ns). The longest, but least reliable, time constant is observed for the amplitude changes in the band at 957 cm^{-1} (40–300 ns). Because the errors associated with these values overlap, these differences are not significant and the intensity changes probably reflect the same structural alteration within the retinal. These PTR/CARS data do not support the possibility that structural changes in retinal occur on different time scales and, therefore, that more than one ns/K-590 intermediate is present.

Four other values for the time constant describing the ps/ns K-590 transformation have been proposed from vibrational measurements.

1. A time constant in the range of 50–250 ns has been reported from the comparison of RR spectra at 10 ps, 6 ns, and 2 μs (Lohrmann et al., 1995; Althaus et al., 1995). This range is in reasonable agreement with the 40–70-ns time constant found in this work.

2. A value of 10 ns has been derived from time-resolved, dispersive IR spectroscopy and a single-value decomposition analysis (Sasaki et al., 1995). Because the instrumental response time in that study is 60 ns, an erroneous estimation of the ns/K-590 (KL) rise time may have been made.

3. From step-scan FTIR spectra, a 400-ns rise time has been attributed to movements of Asp-96 and Asp-115, and a 2-μs decay time has been correlated to changes close to the Schiff-base. In addition, a time constant of 20 ns has been reported and assigned to motion near Asp-115 (Hage et al., 1996). This latter time constant is hydration dependent.

4. A process occurring with a time constant of 5.5 ns has been revealed by picosecond time-resolved fluorescence measurements (Delaney et al., 1993). The decrease in the relative yield of fluorescence shows that the population of the excited electronic state created by optical excitation of K-590 decreases with a 5.5-ns time constant. Because these fluorescence data monitor an excited electronic state process, it is not anticipated that an analogous time constant is to be found from PTR/CARS measurements that monitor the ground electronic state. The excited electronic state relaxation apparently precedes the ps/ns K-590 transformation described here.

Structural alteration of retinal during the ps/ns K-590 transformation

The changes in the vibrational degrees of freedom during the ps/ns K-590 transformation directly reflect movements of the chromophore after its principal all-*trans* to 13-*cis* isomerization. Many of these bands either are assigned to modes close to the Schiff base nitrogen (i.e., 805 cm^{-1}, 957 cm^{-1}, 984 cm^{-1}) or are sensitive to Schiff base nitrogen deuteration (i.e., 952 cm^{-1} and 1362 cm^{-1}), thus also indicating modes close to the Schiff base. That is also valid for the vibrational modes assignable to the bands at 1293 cm^{-1} and 1379 cm^{-1}, the involvement of which in the ps/ns K-590 transformation is unclear. The structural changes in the retinal chromophore occurring in the nanosecond time regime are essentially located in the Schiff base region.

Additionally, smaller alterations occur that involve the middle of the retinal chain near the C_{11}=C_{12} double bond ($C_{11,12}$-HOOP modes at 855 cm^{-1} and 938 cm^{-1}) and that part near the β-ionone ring (C_7 in-plane rocking mode at 1327 cm^{-1}). The band at 1300 cm^{-1} has not been assigned, but because this band is not sensitive to deuteration of the Schiff base nitrogen, its involvement in the transformation supports the presence of alterations of the retinal other than in the Schiff base region. Changes in fingerprint bands (i.e., C-C stretching modes at 1196 cm^{-1}) cannot be correlated with a localized movement of the chromophore because of the highly coupled character of the C-C stretching modes themselves (bands at 1196 cm^{-1}, 1188 cm^{-1}, and 1206 cm^{-1}) (Jäger et al., 1996). It is likely that these changes reflect global alterations along the whole polyene chain.

The general structure of the retinal in ps/K-590 is well known from vibrational spectroscopy. Its principal geome-

try is the 13-*cis* configuration (e.g., Dobler et al., 1988; Mathies et al., 1988; Kandori et al., 1993). The geometry of ps/K-590, however, is not planar, but highly twisted along the polyene chain (Hsieh et al., 1981, 1983; Stern and Mathies, 1985; Brack and Atkinson, 1989; Doig et al., 1991; Lohrmann et al., 1995; Althaus et al., 1995; Ujj et al., 1996). The precise configuration at the C_{14}-C_{15} bond remains under investigation (e.g., Schulten and Tavan, 1978; Gerwert and Siebert, 1986; Smith et al., 1986; Grossjean et al., 1990; Xu et al., 1996; Jäger et al., 1996).

Because the intensities of HOOP modes are directly related to the degree of torsional twisting around specific bonds (Fahmy et al., 1989; Curry et al., 1985), the intensity of bands assigned to these modes provides a detailed view of the out-of-plane retinal motion. The decrease in the C_{11}-C_{12}-HOOP mode (938 cm^{-1}) indicates that ns/K-590 is less twisted in the central C=C-C region than in ps/K-590. The appearance of a new, strong 15-HOOP mode (984 cm^{-1}), together with the intensity decrease in the structurally related mode at 957 cm^{-1}, indicates that large structural rearrangements occur in the terminal part of the retinal near its Schiff base linkage to the protein.

The changes in the chromophore motion during the ps/ns K-590 transformation also reflect modifications in the retinal/protein interaction and/or alterations in the adjacent protein environment. A simple picture describes the transformation as a relaxation process of the retinal. This process would represent the completion of all-*trans* to 13-*cis* isomerization, which is sterically restricted within the physical constraints of the retinal binding pocket. Conceptually, the relaxation may be paralleled by slight movements of specific amino acid side chains close to the retinal. Alternatively, the retinal chromophore motions may be driven by conformational changes in the protein environment. In both cases, changes in the protein environment would occur more slowly than the all-*trans* to 13-*cis* isomerization within the chromophore. Protein alterations have been found to appear during the initial picosecond interval of the RT/BR photocycle (Diller et al., 1991, 1995). The protein conformation itself remains unchanged between 10 ps and 14 ns (Diller et al., 1992), thereby indicating the absence of larger protein alterations during the lifetime of ps/K-590. Protein alterations may be involved in the ps/ns K-590 transformation, but remain to be characterized.

In the ns/K-590 (KL) to L-550 transition, protein structural changes are accompanied by a further relaxation of the retinal structure along its whole chain, except for its highly twisted geometry near the Schiff base linkage (Fahmy et al., 1991; Weidlich and Siebert, 1993). These processes are thought to obtain the prerequisite geometrical and electrostatic driving forces from within the retinal structure itself and from the steric and electrostatic interactions between retinal and the adjacent protein that are associated with deprotonation of the Schiff base during the L-550 to M-412 transition.

CONCLUDING REMARKS

This study reveals the existence of a ps/K-590 to ns/K-590 transformation that involves structural changes in the retinal chromophore of BR with a time constant of 40–70 ns (17°C). No retinal structural changes occur over the 50-ps to 1-ns time regime. Whereas the whole retinal is involved in this transformation, the primary changes are located in the terminal part of the retinal near the Schiff base linkage. An especially strong twist of the C_{14}-C_{15} bond is accompanied by a more planar geometry in the middle part of the retinal polyene chain near the C_{11}=C_{12} bond, and a slightly changed geometry in that part near the β-ionone ring. Alterations of the adjacent protein environment may be included in the transformation, but the involvement of specific amino acids remains to be identified.

The authors thank Mr. J. Rowley, Ms. M. MacDonald, and Mr. I. Malagon for technical assistance. The authors also thank Dr. F. Siebert for stimulating discussions.

This work is supported by a grant to GHA from the National Institutes of Health. FJ gratefully acknowledges a DAAD/NATO fellowship and support from the University of Arizona Foundation.

REFERENCES

Althaus, T., W. Eisfeld, R. Lohrmann, and M. Stockburger. 1995. Application of raman spectroscopy to retinal proteins [review]. *Isr. J. Chem.* 35:227–251.

Ames, J. B., and R. A. Mathies. 1990. The role of back-reactions and proton uptake during the N → O transition in bacteriorhodopsin's photocycle: a kinetic resonance Raman study. *Biochemistry.* 29: 7181–7190.

Atkinson, G. H. 1990. Picosecond reaction dynamics in photosynthetic and proton pumping systems: picosecond time-resolved Raman spectroscopy of electronic and vibrationally excited states. *SPIE.* 1403:50–58.

Atkinson, G. H., T. L. Brack, D. Blanchard, and G. Rumbles. 1989. Picosecond time-resolved resonance Raman spectroscopy of the initial *trans* to *cis* isomerization in the bacteriorhodopsin photocycle. *Chem. Phys.* 131:1–15.

Atkinson, G. H., A. Popp, and L. Ujj. 1994. Picosecond-Resonance Coherent Anti-Stokes Raman Scattering in Biophysics: Power Dependence in the Bacteriorhodopsin Photocycle, Vol. 74. A. Lau, F. Siebert, and W. Werncke, editors. Springer-Verlag, Berlin. 153–157.

Atkinson, G. H., and L. Ujj. 1992. Picosecond Time-Resolved Resonance CARS of Bacteriorhdopsin. *In* Institute of Physics Conference Series, no. 126, section VIII. IOP Publishing. 599–604.

Birge, R. R. 1990. Nature of the primary photochemical events in rhodopsin and bacteriorhodopsin. *Biochim. Biophys. Acta.* 1016:293–327.

Bitting, H. C., D.-J. Jang, and M. A. El-Sayed. 1990. On the multiple cycles of bacteriorhodopsin at high pH. *Photochem. Photobiol.* 51: 593–598.

Blanchard, D., D. A. Gilmore, T. L. Brack, H. Lemaire, D. Hughes, and G. H. Atkinson. 1991. Picosecond time-resolved absorption and fluorescence in the bacteriorhodopsin photocycle: vibrationally-excited species. *Chem. Phys.* 156:155–170.

Brack, T. L., and G. H. Atkinson. 1989. Picosecond time-resolved resonance raman spectrum of the K-590 intermediate in the room temperature bacteriorhodopsin photocycle. *J. Mol. Struct.* 289–303.

Brack, T. L., and G. H. Atkinson. 1991. Vibrationally excited retinal in the bacteriorhodopsin photocycle: picosecond time-resolved anti-Stokes resonance Raman scattering. *J. Phys. Chem.* 95:2352–2356.

Braiman, M. 1986. Resonance Raman methods for proton translocation in bacteriorhodopsin. *Methods Enzymol.* 127:587–597.

Braiman, M. S., O. Bousche, and K. J. Rothschild. 1991. Protein dynamics in the bacteriorhodopsin photocycle: submillisecond Fourier transform infrared spectra of the L, M, and N photointermediates. *Proc. Natl. Acad. Sci. USA.* 88:2388–2392.

Braiman, M., and R. A. Mathies. 1982. Resonance Raman spectra of bacteriorhodopsin's primary photoproduct: evidence for a distorted 13-*cis* retinal chromophore. *Proc. Natl. Acad. Sci. USA.* 79:403–407.

Braiman, M., and R. A. Mathies. 1983. Structural relaxation of the Schiff base bond in bacteriorhodopsin's primary photoproduct. *Biophys. J.* 41:14a.

Curry, B., I. Palings, A. D. Brock, J. A. Pardoen, J. Lugtenburg, and R. Mathies. 1985. Vibrational analysis of the retinal isomers. *In* Advances in Infrared and Raman Spectroscopy, Vol. 12. John Wiley and Sons, New York. 115–178.

Dáncshazy, Z., R. Govindjee, and T. G. Ebrey. 1988. Independent photocycles of the spectrally distinct forms of bacteriorhodopsin. *Proc. Natl. Acad. Sci. USA.* 85:6358–6361.

Delaney, J. K., T. L. Brack, and G. H. Atkinson. 1993. Time-resolved absorption and fluorescence from the bacteriorhodopsin photocycle in the nanosecond time regime. *Biophys. J.* 64:1512–1519.

Diller, R., M. Iannone, R. A. Bogomolni, and R. M. Hochstrasser. 1991. Ultrafast infrared spectroscopy of bacteriorhodopsin. *Biophys. J.* 60: 286–289.

Diller, R., M. Iannone, B. R. Cowen, S. Maiti, R. A. Bogomolni, and R. M. Hochstrasser. 1992. Picosecond dynamics of bacteriorhodopsin, probed by time-resolved infrared spectroscopy. *Biochemistry.* 31:5567–5572.

Diller, R., S. Maiti, G. C. Walker, B. R. Cowen, R. Pippenger, R. A. Bogomolni, and R. M. Hochstrasser. 1995. Femtosecond time-resolved infrared laser study of the J-K transition of bacteriorhodopsin. *Chem. Phys. Lett.* 241:109–115.

Dobler, J., W. Zinth, W. Kaiser, and D. Oesterhelt. 1988. Excited-state reaction dynamics of bacteriorhodopsin studied by femtosecond spectroscopy. *Chem. Phys. Lett.* 144:215–220.

Doig, S. J., P. J. Reid, and R. A. Mathies. 1991. Picosecond time-resolved resonance Raman spectroscopy of bacteriorhodopsin's J, K, and KL intermediates. *J. Chem. Phys.* 95:6372–6379.

Ebrey, T. G. 1993. Light Energy Transduction in Bacteriorhodopsin. M. B. Jackson, editor. CRC Press, Boca Raton, FL. 353–387.

Eisfeld, W., R. Diller, C. Pusch, R. Lohrmann, and M. Stockburger. 1993. Resonance Raman and optical transient studies on the proton pump of bacteriorhodopsin reveal parallel photocycles. *Biochemistry.* 32: 7196–7215.

Fahmy, K., F. Siebert, M. F. Grossjean, and P. Tavan. 1989. Photoisomerization in bacteriorhodopsin studied by FTIR, linear dichroism and photoselection expierments combined with quantum chemical theoretical analysis. *J. Mol. Struct.* 214:257–288.

Fahmy, K., F. Siebert, and P. Tavan. 1991. Structural investigation of bacteriorhodopsin and some of its photoproducts by polarized Fourier transform infrared spectroscopic methods—difference spectroscopy and photoselection. *Biophys. J.* 60:989–1001.

Gerwert, K., and F. Siebert. 1986. Evidence for light-induced 13-cis, 14-cis isomerization in bacteriorhodopsin obtained by FTIR difference spectroscopy using isotopically labelled retinals. *EMBO J.* 5:805–811.

Grossjean, M. F., P. Tavan, and K. Schulten. 1990. Quantum chemical vibrational analysis of the chromophore of bacteriorhodopsin. *J. Phys. Chem.* 94:8059–8069.

Hage, W., M. Kim, H. Frei, and R. A. Mathies. 1996. Protein dynamics in the bacteriorhodopsin photocycle: a nanosecond step-scan FTIR investigation of the KL to L transition. *J. Phys. Chem.* 100:16026–16033.

Hanamoto, J. H., P. Dupuis, and M. A. El-Sayed. 1984. On the protein (tyrosine)-chromophore (protonated Schiff base) coupling in bacteriorhodopsin. *Proc. Natl. Acad. Sci. USA.* 81:7083–7087.

Hessling, B., G. Souvignier, and K. Gerwert. 1993. A model-independent approach to assigning bacteriorhodopsin's intramolecular reactions to photocycle intermediates. *Biophys. J.* 65:1929–1941.

Hsieh, C.-L., M. A. El-Sayed, M. Nicol, M. Nagumo, and J.-H. Lee. 1983. Time-resolved resonance Raman spectroscopy of the bacteriorhodopsin photocycle on the picosecond and nanosecond time scales. *Photochem. Photobiol.* 38:83–94.

Hsieh, C.-L., M. Nagumo, M. Nicol, and M. A. El-Sayed. 1981. Picosecond and nanosecond resonance Raman studies of bacteriorhodopsin. Do configurational changes of retinal occur in picoseconds? *J. Phys. Chem.* 85:2714–2717.

Jäger, F., L. Ujj, G. H. Atkinson, M. Sheves, and M. Ottolenghi. 1996. Vibrational spectrum of K-590 containing $^{13}C_{14,15}$ retinal: picosecond time-resolved Coherent anti-Stokes Raman spectroscopy of the room temperature bacteriorhodopsin photocycle. *J. Phys. Chem.* 100: 12066–12075.

Kandori, H., K. Yoshihara, H. Tomioka, H. Sasabe, and Y. Shichida. 1993. Comparative study of primary photochemical events of two retinal proteins, bacteriorhodopsin and halorhodopsin, by use of subpicosecond time-resolved spectroscopy. *Chem. Phys. Lett.* 211:385–391.

Kochendörfer, G. G., and R. A. Mathies. 1995. Ultrafast spectroscopy of rhodopsins—photochemistry at its best! *Isr. J. Chem.* 35:211–226.

Krebs, M. P., and H. G. Khorana. 1993. Mechanism of light-dependent proton translocation by bacteriorhodopsin. *J. Bacteriol.* 175:1555–1560.

Lanyi, J. K., and G. Váró. 1995. The photocycles of bacteriorhodopsin. *Isr. J. Chem.* 35:365–386.

Lohrmann, R., T. Althaus, W. Eisfeld, and M. Stockburger. 1995. Light-induced reaction sequence of the chromophore in bacteriorhodopsin studied by time-resolved RR spectroscopy. *In* Time-Resolved Vibrational Spectroscopy VI, Vol. 74. A. Lau, F. Siebert, and W. Werncke, editors. Springer-Verlag, Berlin. 208–214.

Lohrmann, R., I. Grieger, and M. Stockburger. 1991. Resonance Raman studies on the intermediate K-590 in the photocycle of bacteriorhodopsin. *J. Phys. Chem.* 95:1993–2001.

Lohrmann, R., and M. Stockburger. 1992. Time-resolved resonance Raman studies of bacteriorhodopsin and its intermediates K_{590} and L_{550}: biological implications. *J. Raman Spectrosc.* 23:575–583.

Lozier, R. H., A. Xie, J. Hofrichter, and G. M. Clore. 1992. Reversible steps in the bacteriorhodopsin photocycle. *Proc. Natl. Acad. Sci. USA.* 89:3610–3614.

Maeda, A. 1995. Application of FTIR spectroscopy to the structural study on the function of bacteriorhodopsin. *Isr. J. Chem.* 35:387–400.

Maeda, A., J. Sasaki, J. Pfefferle, Y. Shichida, and T. Yoshizawa. 1991. Fourier transform infared spectral studies on the Schiff base mode of all-*trans* bacteriorhodopsin and its photointermediates, K and L. *Photochem. Photobiol.* 54:911–921.

Mathies, R. A., C. H. Cruz, W. T. Pollard, and C. V. Shank. 1988. Direct observation of the femtosecond excited-state *cis-trans* isomerization in bacteriorhodopsin. *Science.* 243:777–779.

Mathies, R. A., S. W. Lin, J. B. Ames, and W. T. Pollard. 1991. From femtoseconds to biology: mechanism of bacteriorhodopsin's light-driven proton pump. *Annu. Rev. Biophys. Biophys. Chem.* 20:491–518.

Milder, S., and D. S. Kliger. 1988. A time-resolved spectral study of the K and KL intermediates of bacteriorhodopsin. *Biophys. J.* 53:465–468.

Nölker, K., O. Weidlich, and F. Siebert. 1992. Chromophore and protein reactions of bacteriorhodopsin studied by sub-microsecond time-resolved step-scan FTIR spectroscopy. *In* Time-Resolved Vibrational Spectroscopy V, Vol. 68. H. Takahashi, editor. Springer-Verlag, Berlin. 57–60.

Nuss, M. C., W. Zinth, W. Kaiser, E. Kolling, and D. Oesterhelt. 1985. Femtosecond spectroscopy of the first events of the photochemical cycle in bacteriorhodopsin. *Chem. Phys. Lett.* 117:1–7.

Oesterhelt, D., and W. Stoeckenius. 1974. Isolation of the cell membrane of *Halobacterium halobium* and its fraction into red and purple membrane. *Methods Enzymol.* 31:667–668.

Oesterhelt, D., J. Tittor, and E. Bamberg. 1992. A unifying concept for ion translocation in retinal proteins. *J. Bioenerg. Biomembr.* 24:181–191.

Petrich, J. W., J. Breton, J. L. Martin, and A. Antonetti. 1987. Femtosecond absorption spectroscopy of light-adapted and dark-adapted bacteriorhodopsin. *Chem. Phys. Lett.* 137:369–375.

Polland, H.-J., M. A. Franz, W. Zinth, W. Kaiser, E. Kolling, and D. Oesterhelt. 1986. Early picosecond events in the photocycle of bacteriorhodopsin. *Biophys. J.* 49:651–662.

Popp, A., L. Ujj, and G. H. Atkinson. 1996. Bathorhodopsin structure in the room-temperature rhodopsin photosequence: picosecond time-resolved Coherent anti-Stokes Raman scattering. *Proc. Natl. Acad. Sci. USA.* 93:372–376.

Rothschild, K. J. 1992. FTIR difference spectroscopy of bacteriorhodopsin: toward a molecular model. *J. Bioenerg. Biomembr.* 24:147–167.

Rothschild, K. J., J. Gillespie, and P. Roepe. 1985. Fourier transform infrared spectroscopic evidence for the existence of two conformations of the bacteriorhodopsin primary photoproduct at low temperature. *Biochim. Biophys. Acta.* 808:140–148.

Rothschild, K. J., and H. Marrero. 1982. Infrared evidence that the Schiff base of bacteriorhodopsin is protonated. *Proc. Natl. Acad. Sci. USA.* 79:4045–4049.

Sasaki, J., A. Maeda, C. Kato, and H. Hamaguchi. 1993. Time-resolved infared spectral analysis of the KL-to-L conversion in the photocycle of bacteriorhodopsin. *Biochemistry.* 32:867–871.

Sasaki, J., T. Yuzawa, H. Kandori, A. Maeda, and H. Hamaguchi. 1995. Nanosecond time-resolved infared spectroscopy distinguishes two K species in the bacteriorhosopsin photocycle. *Biophys. J.* 68:2073–2080.

Schulten, K., and P. Tavan. 1978. A mechanism for the light driven proton pump of *Halobacterium halobium. Nature.* 272:85–86.

Sharkov, A. V., A. V. Pakulev, S. V. Chekalin, and Y. A. Matveetz. 1996. Primary events in bacteriorhodopsin probed by subpicosecond spectroscopy. *Biochim. Biophys. Acta.* 808:94–102.

Shichida, Y., S. Matuoka, Y. Hidaka, and T. Yoshizawa. 1983. Absorption spectra of intermediates of bacteriorhodopsin measured by laser photolysis at room temperatures. *Biochim. Biophys. Acta.* 723:240–246.

Siebert, F., and W. Mäntele. 1983. Investigation of the primary photochemistry of bacteriorhodopsin by low-temperature Fourier-transform infrared spectroscopy. *Eur. J. Biochem.* 130:565–573.

Smith, S. O. 1985. Resonance Raman studies on the mechanism of proton translocation by bacteriorhodopsin's retinal chromophore. Thesis, California State University.

Smith, S. O., M. Braiman, and R. A. Mathies. 1983. Time-resolved resonance Raman spectroscopy of the K-610 and O-640 photointermediates of bacteriorhodopsin. *In* Time-Resolved Vibrational Spectroscopy. G. H. Atkinson, editor. Academic Press, New York. 219–230.

Smith, S. O., I. Hornung, R. Van Der Steen, J. A. Pardoen, M. Braiman, J. Lugtenburg, and R. A. Mathies. 1986. Are C_{14}-C_{15} single bond isomerizations of the retinal chromophore involved in the proton-pumping mechanism of bacteriorhodopsin? *Proc. Natl. Acad. Sci. USA.* 83: 967–971.

Stern, D., and R. A. Mathies. 1985. Picosecond and nanosecond resonance Raman evidence for structural relaxation in bacteriorhodopsin's primary photoproduct. *In* Springer Proceedings in Physics 4. A. Laubereau and M. Stockburger, editors. Springer-Verlag, Berlin. 250–254.

Stockburger, M., T. Alshuth, D. Oesterhelt, and W. Gärtner. 1986. Resonance Raman Spectroscopy of Bacteriorhodopsin: Structure and Function. R. J. Clark and R. E. Hester, editors. John Wiley and Sons, New York. 483–535.

Terner, J., C.-L. Hsieh, A. R. Burns, and M. A. El-Sayed. 1979. Time-resolved resonance Raman spectroscopy of intermediates of bacteriorhodopsin: the bK_{590} intermediate. *Proc. Natl. Acad. Sci. USA.* 76:3046–3050.

Uhmann, W., A. Becker, C. Taran, and F. Siebert. 1991. Time-resolved FT-IR absorption spectroscopy using a step-scan interferometer. *Appl. Spectrosc.* 45:390–397.

Ujj, L., F. Jäger, A. Popp, and G. H. Atkinson. 1996. Vibrational spectrum of the K-590 intermediate in the bacteriorhodopsin photocycle at room temperature: picosecond time-resolved resonance Coherent anti-Stokes Raman spectroscopy. *Chem. Phys.* 212:421–436.

Ujj, L., A. Popp, and G. H. Atkinson. 1994a. Picosecond resonance Coherent anti-Stokes Raman spectroscopy of bacteriorhodopsin: quantitative third-order susceptibility analysis of the dark-adapted mixture. *Chem. Phys.* 188:221–234.

Ujj, L., B. L. Volodin, A. Popp, J. K. Delaney, and G. H. Atkinson. 1994b. Picosecond resonance Coherent anti-Stokes Raman spectroscopy of bacteriorhodopsin: spectra and quantitative third-order susceptibility analysis of the light-adapted BR-570. *Chem. Phys.* 182:291–311.

van den Berg, R., H. C. Bitting, and M. A. El-Sayed. 1990. Subpicosecond resonance Raman spectra of the early intermediates in the photocycle of bacteriorhodopsin. *Biophys. J.* 58:135–141.

Váró, G., and J. K. Lanyi. 1991. Kinetic and spectroscopic evidence for an irreversible step between deprotonation and reprotonation of the Schiff base in the bacteriorhodopsin photocycle. *Biochemistry.* 30:5008–5015.

Weidlich, O., and F. Siebert. 1993. Time-resolved step-scan FT-IR investigations of the transition from KL to L in bacteriorhodopsin photocycle: identification of chromophore twists by assigning hydrogen-out-of-plane (HOOP) bending vibrations. *Appl. Spectrosc.* 47:1394–1400.

Xu, D., C. Martin, and K. Schulten. 1996. Molecular dynamics study of early picosecond events in the bacteriorhodopsin photocycle: dielectic response, vibrational cooling and the J, K, intermediates. *Biophys. J.* 70:453–460.

Yamamoto, N., T. W. Ebbesen, and H. Ohtani. 1994. Does the KL intermediate exist in the photocycle of bacteriorhodopsin? *Chem. Phys. Lett.* 228:61–65.